Stability, electronic, and optical properties of wurtzite $Cu_2Cd_xZn_{1-x}SnS_4$ alloys as photovoltaic materials: First-principles insight

S. Kumar* and Durgesh Kumar Sharma
Applied Physics Department, Faculty of Engineering and Technology, M. J. P. Rohilkhand University, Bareilly-243 006, India

S. Auluck
CSIR-National Physical Laboratory, Dr. K.S. Krishnan Marg, New Delhi-110 012, India
(Received 7 July 2016; revised manuscript received 14 October 2016; published 19 December 2016)

First-principles calculations have been performed to understand the structural and electronic properties of wurtzite (wz) phase of cation mixed $Cu_2Cd_xZn_{1-x}SnS_4$ (CCZTS) alloys which have a band gap that fits the requirement of a solar cell light absorber. We have used five different exchange correlations (XCs) to fix the structural parameters with high accuracy. The hybrid XC, which has been used to explain thermodynamical, electronic, and optical properties, shows very promising results. We find that (i) the CCZTS alloys are highly miscible with low formation enthalpies, (ii) the band gap of CCZTS alloys can be tuned in the range 1.56–1.39 eV as Cd concentration (x) increases from 0.0 to 1.0 with a small bowing parameter $b = 0.293$ eV, and (iii) the calculated band gap of CCZTS alloys decreases mainly due to the upshift of the valence band. Our predicted results are in agreement with the only available synthesized wz phase CCZTS data [Ramasamy *et al.*, RSC Adv. **3**, 1186 (2013)]. The dependence of the CCZTS alloys energy on growth temperature is also calculated. Our results could be very useful for growth of these materials.

DOI: 10.1103/PhysRevB.94.235206

I. INTRODUCTION

Among the numerous photovoltaic materials, $CuIn_{1-x}Ga_xSe_2$ (CIGSe) alloys have been used to make thin film solar cells [1,2]. This is attributed to the high power conversion efficiency and stability of these alloys. However, in recent years the rising prices of gallium and indium and its limited stock have hampered further development in the field of thin film solar cells [3] of these alloys. Therefore, there is a focus on finding alternate materials comprising of nontoxic and earth abundant elements that could support the photovoltaic industry [4]. The quaternary semiconductor Cu_2ZnSnS_4 (CZTS) and Cu_2CdSnS_4 (CCTS) and its alloy-based solar cells have reached conversion efficiency of about 12%, making them one of the useful candidates in the thin film solar cell industry [5–7]. There is further a possibility to enhance the efficiency of CZTS-based solar cells by the fabrication of multifunctional solar cells.

The CZTS, CCTS, and their $Cu_2Cd_xZn_{1-x}SnS_4$ (CCZTS) alloys are the ideal alternative to commercialized photovoltaic semiconductor CIGSe because they consist of earth abundant elements rather than scarce elements such as In and Ga. Further, the current-voltage (I-V) measurements [8] also suggest that Cd-doped CZTS fit well for solar cell applications. The I-V characteristics show that the photocurrent increases with increasing Cd concentration in CCZTS alloys and it becomes maximum for $x = 0.75$ including end compounds CZTS and CCTS. This clearly confirms the suitability of CCZTS alloys for solar cell applications. However, the material is still under investigation and there is a need for additional exploration experimentally as well as theoretically. The different concentrations of Cd in CCZTS alloys have energy band gaps covering the whole span of the visible solar spectrum which makes them useful for various functions. The multifunctional solar cells of CIGSe, $In_xGa_{1-x}P$, and $In_xGa_{1-x}As$ have been fabricated because the tunable band gap can be controlled by the In concentration [2,9–11]. Therefore, it is important to understand the energy band gap variation in materials based on CCZTS for making low cost tandem solar cells. Furthermore, the band offset at the interface is an important physical parameter which is used to assess interface effects for the design of solar cells. The knowledge of band offset at the interface is very helpful in the design of optoelectronic devices. To understand the above properties one needs an accurate description of the energy band structure and how the valence band maxima (VBM) and conduction band minima (CBM) shift in CCZTS alloys as a function of Cd concentration.

Xio *et al.* [12] synthesized the kesterite phase of CCZTS alloys and showed that the energy band gap of CCZTS alloys can be tuned in the range of 1.55–1.09 eV by changing the Cd concentration. This suggests that the CCZTS is a potentially suitable material for fabrication of future light efficient multifunctional solar cells. Walsh *et al.* [13] performed a first-principles calculation of kesterite phase CZTS and also studied the effect of replacing S by Se in $Cu_2ZnSn(S_{1-x}Se_x)_4$ (CZTSSe) alloys to understand the electronic structure, phase stability, and defect properties. The energy band gap variation with Se concentration has been explained on the basis of band offset. Wei *et al.* [14] have investigated the wz structure along with zinc-blende (zb) -derived kesterite structures and concluded that the energy band gaps of wz-derived structures are relatively larger than those of a zb structure. Ramasamy *et al.* [8] have synthesized the wz phase of CCZTS alloys over the entire range of Cd contents from $x = 0.00$ to 1.00. The

*skumar@mjpru.ac.in; drsudhirkumar.in@gmail.com

measured band gap decreases almost linearly from 1.56 eV ($x = 0.00$) to 1.39 eV ($x = 1.00$). The measured photocurrent maxima for $x = 0.75$ indicates that doping of Cd into CZTS enhances photogenerated carrier concentration.

Looking into the above reports, we note that a detailed theoretical study of wz CCZTS alloys has never been performed. Therefore it becomes of utmost importance to have a complete and clear understanding of the electronic structure and other related properties of these alloys. We hope that the present study will help to fill the gap between theoretical and experimental work and can help to improve solar cell performance.

In Sec. II, we give the details of the computational work. Section III is devoted to results and discussion of the structural parameters, miscibility, band gap bowing, and band offsets. Our conclusions are summarized in Sec. IV.

II. COMPUTATIONAL DETAILS

We have used the density functional theory (DFT) based plane wave Vienna *ab initio* Simulation Package (VASP) [15,16] to calculate the electronic properties. The core valence interactions are treated within the projector augmented wave scheme [17]. The *d* states of groups II and IV elements are treated explicitly as a valence band. A plane wave cutoff equal to 500 eV was used and a Brillouin zone (BZ) sample at the zone center with smearing width $\sigma = 0.05$ eV. For BZ integration, we have used *k*-point meshes that are equivalent to 4×4×4 Monkhorst-Pack mesh for the end compound, and 2×2×2 *k*-point mesh for the 64-atom supercell of CCZTS alloys. All lattice vectors and atomic positions were fully relaxed by minimizing the quantum-mechanical stress and the Hellmann-Feynman forces on each atom became smaller than 0.01 eV/Å.

In spite of certain deficiencies in the generalized gradient approximations (GGAs) [18], we performed GGA calculations which give energy band gaps 0.02 and 0.12 eV for CZTS and CCTS, respectively. This shows that the energy band gap calculated with GGA is heavily underestimated indicating that GGA is not suitable for band offset study of CCZTS alloys. Therefore, we have decided to switch over to hybrid functional calculations. In order to overcome the semilocal description of XC for the study of electronic properties, we employed the Heyd, Scuseria, and Ernzerhof (HSE06) [19] functional. In HSE06 XC the standard value of screening and the mixing parameter (α) set to 0.20 $Å^{-1}$ and 0.25, respectively. The HSE06 functional predicts better bandwidths, total energy, and energy band gaps in comparison to GGA. However, the standard HSE06 functional predicts the energy band gaps for end compounds CZTS and CCTS equal to 0.45 and 0.25 eV, respectively. This suggests that an overscreening of exchange interaction with a standard value of $\alpha = 0.25$ gives smaller energy band gaps compared to the experimental values. Therefore, there is a need to improve the calculated energy band gaps. We found that by increasing α equal to 0.51 makes the calculated band gaps match the experimental values [8]. It will also improve the electronic, optical, and band offset properties. In the present calculations we have used a mixing parameter equal to 0.51, therefore we use the term HSE instead of HSE06. The screening parameter is kept constant throughout this work. It may be noted that the electronic properties obtained using HSE have been previously proved to be very successful [20].

TABLE I. Total number of configurations (C_T) and number of symmetrically inequivalent configurations (C) calculated for $Cu_2Cd_xZn_{1-x}SnS_4$ alloys.

Supercell	Concentration (x)	C_T	C
2×2×1	0.25	28	10
2×2×1	0.50	70	22
2×2×1	0.75	28	10

The CCZTS alloy was modeled using a 2×2×1 supercell of the conventional wz crystal structure. In the 64-atom supercell Cd/Zn atoms occupy eight distinct lattice sites. Therefore the total number of configurations for the Cd-doped CZTS supercell is in principle equal to ${}^8C_2 = 28$ for $x = 0.25$ and 0.75 and ${}^8C_4 = 70$ for $x = 0.50$. Out of the total possible configurations (C_T), the symmetrically inequivalent configurations were calculated by using the site occupancy disorder (SOD) [21] program. This gives ten distinct configurations (C) for $x = 0.25$ and 0.75 and 22 for $x = 0.50$, respectively. This is to confirm that the number of inequivalent configurations is drastically reduced when the symmetry of the lattice is taken into account (see Table I). We have calculated the total energy of all the distinct configurations for pristine CZTS and CCTS along with CCZTS alloys and these are presented in Fig. 1. It is clear that at the high energy end, the density of configurations decreases for all cases. For further calculations of the electronic properties of CCZTS alloys we have used only the most stable configuration as a representative for each composition. We have also performed Boltzmann probability analysis for the CCZTS alloys. This shows that the probability decreases rapidly with increasing temperature for all three concentrations $x = 0.25$, 0.50, and 0.75. To draw any final conclusion about the phase transformation with temperature one needs large supercell calculations, which is beyond the scope of the present paper.

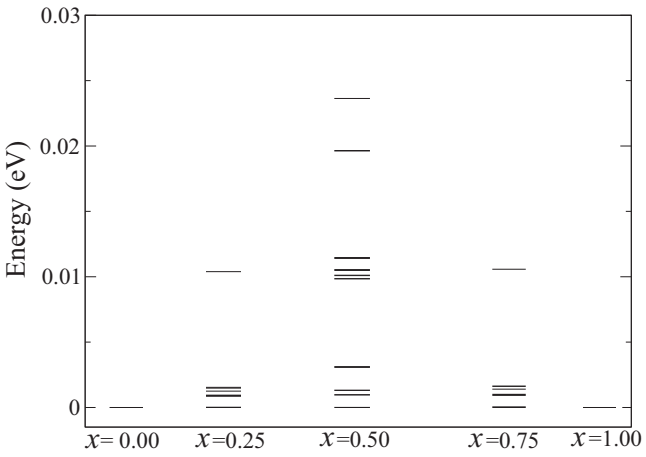

FIG. 1. The calculated configurational energies (relative to lowest energy for each composition) of relaxed inequivalent configurations generated by SOD for $Cu_2Cd_xZn_{1-x}SnS_4$ alloys using GGA.

TABLE II. Calculated structural parameters (in Å) along with experimental values of $Cu_2Cd_xZn_{1-x}SnS_4$ alloys.

	Calculated lattice constants											
	LDA		GGA		PBESol		AM05		DFT-D_3		Experimental[a]	
Conc. (x)	a	c	a	c	a	c	a	c	a	c	a	c
0.00	3.78	6.12	3.88	6.30	3.81	6.22	3.81	6.23	3.87	6.33	3.825	6.318
0.25	3.78	6.22	3.88	6.39	3.82	6.29	3.82	6.30	3.88	6.39	3.848	6.371
0.50	3.80	6.25	3.91	6.42	3.84	6.31	3.85	6.32	3.91	6.42	3.865	6.374
0.75	3.82	6.29	3.92	6.46	3.86	6.35	3.87	6.37	3.92	6.33	3.919	6.422
1.00	3.86	6.23	3.97	6.45	3.91	6.31	3.91	6.32	3.96	6.45	3.926	6.451

[a]Ref. [8].

III. RESULTS AND DISCUSSION

A. Structural parameters

Defect calculations using DFT to predict the structural and electronic properties are quite challenging. The first major task is to choose an appropriate XC for the calculations. To find out accurate lattice constants of CCZTS alloys, we have used five different XC functionals and the obtained lattice constants are presented in Table II along with the available experimental data.

As a base calculation, we used the simplest local density approximation (LDA) [22]. It is well known that for most cases, this underestimates the lattice parameter and gives overbinding. Our calculated lattice constants, presented in Table II, are as per our expectations. The most widely used semilocal GGA functionals given by Perdew-Burke-Ernzerhof (PBE) [18], improves upon the LDA by including the density gradient $\Delta n(r)$. GGA functionals improve the total energy and lengthen the bonds resulting in an overestimate of the lattice constants. The new PBESol [23] gives a better equation of state closer to the experimental value than LDA/GGA. The lattice constants calculated using PBESol (measured) are 3.81 (3.82) and 6.22 (6.31) Å for the end compounds. We note that the AM05 functional gives lattice constants similar to the PBESol except for a slight improvement in lattice constant towards the z direction.

There is a limitation of (semilocal) DFT functionals in that their poor description of the nonlocal electron correlation gives rise to dispersion (van der Waals) forces. To assess the importance of these dispersion forces, we have used the new Grimme DFT-D_3 [24] functionals which accounts for the change in atomic polarizability, thus allowing the dispersion correlation to be varied based on the atomic coordination environment including three-body as well as pair interactions. The calculated lattice constants using DFT-D_3 [24] overestimates the basal as well as perpendicular lattice constants. The calculated structural parameters using the different XC, as discussed above, are summarized in Table II. Looking at Table II, we see that AM05 is the best choice for the lattice constants and could be used for further calculations.

B. Miscibility

As reported previously [8], the cation mixed wz structures are metastable. Here the Cu, Zn, and Sn atoms occupy one hexagonal-close-packed sublattice while the anions occupy the other sublattice. In Fig. 2, we show the crystal structure which has the lowest energy/atom among all possible structures derived out of SOD [21]. The alloy formation enthalpy (ΔH_f) which is defined as

$$\Delta H_f(x) = E(x) - (1-x)E_{(Cu_2CdSnS_4)} - xE_{(Cu_2ZnSnS_4)}, \quad (1)$$

where $E(x)$ is the total energy of the CCZTS alloys at the composition (x) calculated using a SOD-generated supercell, and $E_{(Cu_2CdSnS_4)}$ and $E_{(Cu_2ZnSnS_4)}$ are the total energy of the CCTS and CZTS, respectively. The $\Delta H_f(x)$ is the energy cost for the mixing Cd and Zn in a certain lattice. The calculated $\Delta H_f(x)$, shown in Fig. 3, indicates that some alloys have a negative value of $\Delta H_f(x)$ depending on the composition parameter (x). The values of $\Delta H_f(x)$ of the wz-derived alloys are always lower than those of the zb structure. The negative value of ΔH_f indicates exothermic reaction during alloys formation which is thermodynamically favorable. Furthermore, the cation mixed alloys, zb-derived $Cu_2(Zn,Fe)SnS_4$, also show a negative value of ΔH_f [25].

To calculate the miscibility temperature, the calculated $\Delta H_f(x)$ (presented in Fig. 3) are fitted to a second order polynomial based on a quasichemical model to get the interaction parameter (Ω) which is an indicator of the alloys solubility and depends on material.

$$\Delta H_f(x) = \Omega x(1-x). \quad (2)$$

The green hexagonal symbol presented in Fig. 3 shows the calculated value of $\Delta H_f(x)$ of wz CCZTS-derived alloys for different concentrations (x) = 0.25, 0.50, and 0.75. Fitting

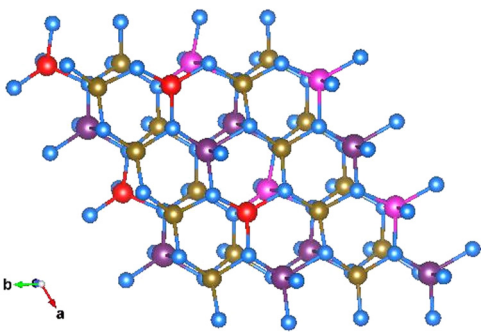

FIG. 2. The SOD-generated crystal structure for $x = 0.50$ where atoms are color coded as follows: gold, Cu; magenta, Cd; red, Zn; violet, Sn; and light blue, S.

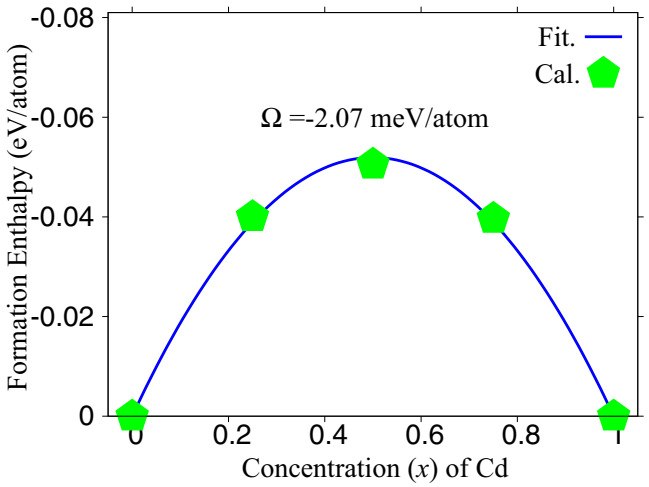

FIG. 3. The calculated formation enthalpy of $Cu_2Cd_xZn_{1-x}SnS_4$ alloys fitted with Eq. (2).

these data according to Eq. (2) gives the interaction parameter $\Omega = -2.07$ meV/atom smaller than anion/cation mixed zb-derived structures such as CZTSSe [26] and $CuIn_xGa_{1-x}Se_2$ [27], suggesting that CCZTS alloys can be easily grown under standard growth temperatures. The size and chemical mismatch between S,Se and Ga,In is larger than that between Cd and Zn. This results in a smaller interaction parameter for CCZTS alloys. In order to mix the cation Cd and Zn, we can analytically estimate the miscibility gap from the behavior as a function of temperature. The mixing Helmholtz free energy (ΔF_m) can be defined as follows:

$$\Delta F_m = \Omega x(1-x) + RT[x\ln x + (1-x)\ln(1-x)]. \quad (3)$$

Thereby the binodal and spinodal decomposition curves can be produced through $\frac{\partial F_m}{\partial x} = 0$ and $\frac{\partial^2 F_m}{\partial x^2} = 0$ and results in Eq. (3) being simplified as follows:

$$RT[\ln x - \ln(1-x)] + (1-2x)\Omega = 0 \quad (4)$$

and

$$RT - 2x(1-x)\Omega = 0. \quad (5)$$

The obtained phase diagram is presented in Fig. 4. In Fig. 4, the binodal and spinodal curves touch at $x = 0.50$ at critical temperature (T_c) 503 K, showing a symmetry feature. However, T_c of CCZTS alloys distinguishes itself from the solar cell materials CIGSe alloys where the calculated [27] interaction parameter and miscibility temperature equal to 176 meV/mixed atom and 1000 K, respectively. The high miscibility temperature results in phase separation which limits the solar cell performance of CIGSe. At a particular temperature below T_c, for example at 400 K, CCZTS alloys can still be formed but with lower solubility, i.e., concentration (x) of Cd should lie within $0 < x < x_1$ or $x_2 < x < 1$, shown in Fig. 4. However, when concentration (x) varies between $x_1 < x < x_2$, the alloys will be unstable and decomposed into more than one phase with the concentrations x_1 and x_2.

C. Band gap bowing

Since the composition tunable CCZTS alloys can be synthesized with good miscibility, we can look at how the composition (x) influences the band gap. The energy band gap of CCZTS alloys can be described by the following equation:

$$E_g = xE_{g(Cu_2CdSnS_4)} + (1-x)E_{g(Cu_2ZnSnS_4)} - bx(x-1), \quad (6)$$

where E_g is the band gap and b is the bowing parameter. The b is obtained by fitting Eq. (6) with a calculated band gap of CCZTS alloys at different concentrations (x). The estimated value of b is small and numerically equal to 0.293 eV, which suggests that the alloys are well behaved. This may be due to the fact that the lattice mismatch between end compounds is less than 1% and the small size difference and chemical difference between Zn and Cd. The small value of the bowing parameter of wz CCZTS shows that the quaternary compounds have good tolerance to the chemical mixed difference of the mixed alloys. The good agreement between the calculated energy band gap and corresponding measured value [8] is presented in Fig. 5. This would be useful for predicting band

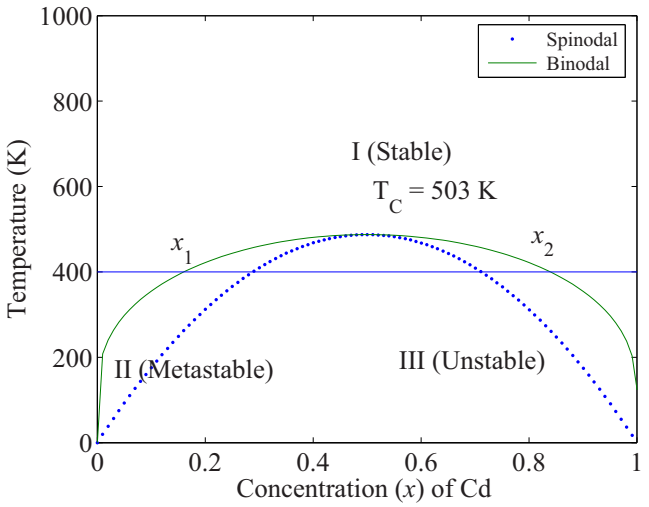

FIG. 4. The calculated miscibility of $Cu_2Cd_xZn_{1-x}SnS_4$ alloys.

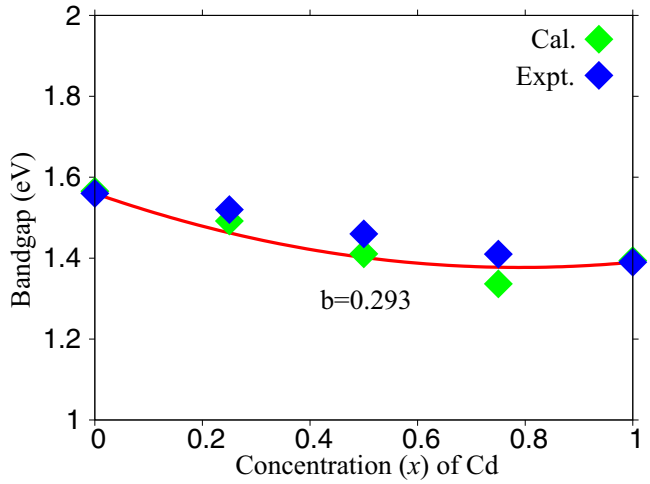

FIG. 5. The calculated band gap for $Cu_2Cd_xZn_{1-x}SnS_4$ alloys along with experimental value (see Ref. [8]).

TABLE III. The concentration (x), energy band gap (E_g) in eV, branch point energy (E_{BP}) in eV, and formation enthalpy (ΔH_f) in eV/atom; ΔE_c and ΔE_v are conduction and valence band discontinuities in eV of $Cu_2Cd_xZn_{1-x}SnS_4$ alloys.

x	E_g^{+} [a]	E_g^{*} [b]	E_{BP}	ΔE_c	ΔE_v	ΔH_f
0.00	1.5656	1.56	4.2006	−2.6350	−4.2006	0.000000
0.25	1.4917	1.52	4.1640	−2.6723	−4.1640	−0.046025
0.50	1.4105	1.46	4.0394	−2.6289	−4.0394	−0.050550
0.75	1.3365	1.41	3.9362	−2.5997	−3.9362	−0.039675
1.00	1.3939	1.39	3.7587	−2.3648	−3.7587	0.000000

[a] E_g^{+}, present with HSE.
[b] E_g^{*}, Ref. [8].

offsets. From Fig. 5, we see that the band gaps for CCZTS alloys decrease with the Cd composition (x) with small bowing. This can be compared with anion mixed CZTSSe [28] which shows a linear decrease in the energy band gap.

D. Band offsets

To understand how the energy band gap decreases with the increasing Cd concentration (x), we will look at the CBM and VBM values. The electronic structure calculation gives the energy eigenvalues at each desired k point of the BZ. The band offsets are calculated using an approach given earlier [29]. The branch point energy (E_{BP}) is calculated by averaging the energy eigenvalues of the highest valence bands (VBs) and lowest conduction bands (CBs) at each desired k point of BZ as follow:

$$E_{BP} = \frac{1}{2N_k}\sum_k \left[\frac{1}{N_{CB}}\sum_i^{N_{CB}} \varepsilon_{c_i}(k) + \frac{1}{N_{VB}}\sum_j^{N_{VB}} \varepsilon_{v_j}(k)\right]. \quad (7)$$

The N_k is the k points at Γ-center of the BZ. We include one lowest CB (i.e., $N_{CB} = 1$) and three uppermost VBs (i.e., $N_{VB} = 3$). We include only one CB in Eq. (7) because the second lowest band shows larger k dispersion throughout the BZ than the lowest one but the same is not true for VBs. The calculated E_{BP} with Eq. (7) is presented in Table III and is used as the universal energy level of reference to align the energy bands of the different concentrations of CCZTS alloys. For all Cu-based chalcogenides including the quaternary and ternary compounds, the VBM is composed of the anion $3p$ and Cu-$3d$ states, while the CBM is composed of S-$3p$ states and Sn-$5s$ states.

The calculated band offsets are shown in Fig. 6. It is clear that the VBM of the CCZTS alloys shift upwards with increasing concentration (x) of Cd by a significant amount. On the other hand, for $x = 0.00$ to 0.75, there is a small change in CBM, while for $x = 1.00$, it shifts upwards by 0.23 eV, which is about half of the VBM upshift. The small CB offsets are because of CBM is dominated by S-$3s$,$3p$ and Sn-$5s$ states. The Sn shows a lower s-orbital energy than the other elements and therefore the substitution of Cd instead of Zn does not affect the CBM energies significantly. On the other hand, the VBM of these compounds consists of S-p and Cu-$3d$ orbitals. The nature of the band offset for common cation alloys can be explained by the positions of the $3d$ orbitals of cations.

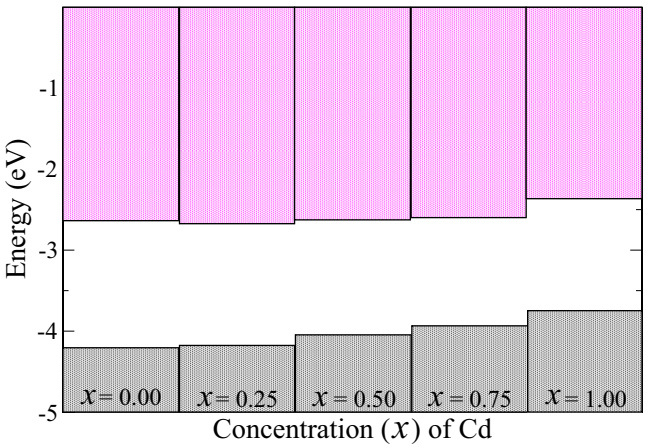

FIG. 6. The calculated band offset of $Cu_2Cd_xZn_{1-x}SnS_4$ alloys.

The energy of the $4d$ states of Cd is higher than that of the $3d$ states of Zn. The shallower cation d orbitals of Cd repel the anion p bands upwards more than the deeper cation $3d$ states of Zn. Thus the VBM of CCZTS shifts upwards with an increase in concentration (x) of Cd. We can further predict the electrical conductivity of these alloys. As per doping rule [30], a material is difficult to be doped p type if the VBM energy is low and difficult to be doped with n type if the CBM is high. The small CB offsets shown in Fig. 6 indicate the intrinsic n-type conductivity should be expected in CCZTS alloys.

IV. CONCLUSIONS

We have investigated the structural, electronic, and thermodynamic properties of CCZTS alloys. The use of HSE hybrid functionals has shown significant improvement in the description of electronic structures including energy band gap and band offsets. Nevertheless the gain in accuracy has been achieved by more than twofold computational cost compared to semilocal DFT. The change in composition (x) of Cd leads to interesting results. We find that the formation enthalpy is small and negative suggesting that Cd can be easily doped and mixed into CCZTS. The small variation in $\Delta H_f(x)$ and lattice constants along with concentration (x) of CCZTS alloys also indicate that it should be easy to grow material with mixed phases depending on the growth method and growth conditions. The band gap dependence on the alloy composition shows a small bowing due to the size and chemical mismatch between Zn and Cd. The decrease in band gap with increasing Cd concentration (x) results primarily from the VBM upshift. Based on these results we can suggest that CCZTS alloys can be synthesized for photovoltaic applications.

ACKNOWLEDGMENTS

This work was supported by the Science and Engineering Research Board (SERB), New Delhi under Grant No. SB/S2/CMP-033/2014. S.A. would like to thank the High Performance Facilities at Intra-University Accelerator Centre (IUAC) at New Delhi, Indian Institute of Mathematical Sciences (IIMSc) at Chennai, CSIR-4PI at Bangaluru, and Indian Institute of Technology at Kanpur.

[1] K. Ramanathan, G. Geeter, J. C. Keane, and R. Nouti, Thin Solid Films **480**, 499 (2005).
[2] M. Schmid, R. Caballero, R. Klenk, J. Krč, T. Rissom, M. Topič, and M. Ch. Lux-Steiner, EPJ Photovoltaics **1**, 10601 (2010).
[3] C. Wadia, A. P. Alivisatos, and D. M. Kammen, Environ. Sci. Technol. **43**, 2072 (2009).
[4] L. M. Peter, Philos. Trans. R. Soc. A **369**, 1840 (2011).
[5] T. K. Todorov, J. Tang, S. Bag, O. Gunawan, Y. Gokmen, T. Zhu and D. B. Mitzi, Adv. Energy Mater. **3**, 34 (2013).
[6] D. A. R. Barkhouse, O. Gunawan, T. Gokmen, T. K. Todorov, and D. B. Mitzi, Prog. Photovoltaics **20**, 6 (2012).
[7] M. T. Winkler, W. Wang, O. Gunawan, H. J. Hovel, T. K. Todorov, and D. B. Mitzi, Energy Environ. Sci. **7**, 1029 (2014).
[8] K. Ramasamy, X. Zhang, R. D. Bennett, and A. Gupta, RSC Adv. **3**, 1186 (2013).
[9] M. Meusel, C. Baur, G. Létay, A. W. Bett, W. Warta, and E. Frenandez, Prog. Photovoltaics **11**, 499 (2003).
[10] N. J. Ekin-Daukes, K. W. J. Barnham, J. P. Connolly, J. S. Roberts, J. C. Clark, G. Hill, and M. Mazzer, Appl. Phys. Lett. **75**, 4195 (1999).
[11] H. K. Kang, S.-H. Park, D. H. Jun, C. Zoo Kim, K. M. Song, W. Park, C. G. Ko, and H. Kim, Semicond. Sci. Technol. **26**, 075009 (2011).
[12] Z.-Y. Xiao, Y.-F. Li, B. Yao, R. Deng, Z.-H. Ding, T. Wu, G. Yang, C.-R. Li, Z.-Y. Dong, L. Liu, L.-G. Zhang, and H.-F. Zhao, J. Appl. Phys. **114**, 183506 (2013).
[13] A. Walsh, S. Chen, S.-H. Wei, and X.-G. Gong, Adv. Energy Mater. **2**, 400 (2012).
[14] S. Chen, A. Walsh, Y. Luo, J.-H. Yang, X. G. Gong, and S.-H. Wei, Phys. Rev. B **82**, 195203 (2010).
[15] G. Kresse and J. Furthmüller, Comput. Mater. Sci. **6**, 15 (1996).
[16] G. Kresse and J. Furthmüller, Phys. Rev. B **54**, 11169 (1996).
[17] P. E. Blöchl, Phys. Rev. B **50**, 17953 (1994).
[18] J. P. Perdew, K. Burke, and M. Ernzerhof, Phys. Rev. Lett. **77**, 3865 (1996).
[19] J. Heyd, G. E. Scuseria, and M. Ernzerhof, J. Chem. Phys. **118**, 8207 (2003).
[20] S. Kumar, S. Joshi, S. K. Gupta, and S. Auluck, J. Phys. D.: Appl. Phys. **49**, 205103 (2016).
[21] R. Grau-Crespo, S. Hamad, C. R. A. Catlow, and N. H. de Leeuw, J. Phys.: Condens. Matter **19**, 256201 (2007).
[22] D. M. Ceperley and B. J. Alder, Phys. Rev. Lett. **45**, 566 (1980).
[23] J. P. Perdew, A. Ruzsinszky, G. I. Csonka, O. A. Vydrov, G. E. Scuseria, L. A. Constantin, X. Zhou, and K. Burke, Phys. Rev. Lett. **100**, 136406 (2008).
[24] S. Grimme, J. Antony, S. Ehrlich, and H. Krieg, J. Chem. Phys. **132**, 154104 (2010).
[25] T. Shibuya, Y. Goto, Y. Kamihara, M. Matoba, K. Yasuoka, L. A. Burton, and A. Walsh, Appl. Phys. Lett. **104**, 021912 (2014).
[26] S. Chen, A. Walsh, J.-H. Yang, X. G. Gong, L. Sun, P.-X. Yang, J.-H. Chu, and S.-H. Wei, Phys. Rev. B **83**, 125201 (2011).
[27] S.-H. Wei and A. Zunger, J. Appl. Phys. **78**, 3846 (1995).
[28] F.-J. Fan, L. Wu, M. Gong, G. Liu, Y.-X. Wang, S.-H. Yu, S. Chen, L.-W. Wang, and X. G. Gong, ACS Nano. **7**, 1454 (2013).
[29] A. Schleif, F. Fuchs, C. Rödl, J. Furthmüller, and F. Bechstedt, Appl. Phys. Lett. **94**, 012104 (2009).
[30] S. B. Zhang, S.-H. Wei, and A. Zunger, J. Appl. Phys. **83**, 3192 (1998).